COPY NO. 2

CR 166264

AERODYNAMICS MEASUREMENTS CONCERNED WITH A TURRET MODEL

(NASA-CR-166264) AERODYNAMIC MEASUREMENTS CONCERNED WITH A TURRET MODEL (Raman Aeronautics Research and) 44 p HC A03/MF A01 CSCL 01A

N82-12034

Unclas G3/02 02229

K. R. Raman

Prepared under Contract No.NAS 2-10579

by

RAMAN AERONAUTICS, INC.

734, Melville Ave.

Palo Alto,CA.

for

NASA / AMES RESEARCH CENTER, MOFFETT FIELD.CA.

TABLE OF CONTENTS

ACKNOWLEDGEMENT

I am grateful for all the help I received during the calibration tests of the five hole probe at the U.S. Air Force Academy, Colorado Springs, CO, from Lt. Col. R.W. Gallington and Mr. F. Jaynes. I have enjoyed discussing every phase of the reported work with Mr. D.A. Buell, his guidance and valuable advice are greatly appreciated.

I would also like to thank Mr. J. Bealkowski for his assistance in reducing all the data through the tedious and intricate spline curve fit program on the HP 9830.

Symbols

M	Mach number
p	Static pressure,N/m^2
p_T	Total pressure,N/m^2
q	Dynamic pressure,N/m^2
Re/m	Reynolds number/meter,1/m
RMS	Root mean square value of the parameter under consideration
T_T	Total temperature,deg.K
$\vec{X}$	Position vector,(x,y,z),m
τ	Time delay,sec
θ	Angular orientation of five hole probe to $\vec{V}$,or aft look azimuth angle,deg.
R	Radial distance from the center of Coelostat turret,m
P(j)	Indicated pressure at various ports of the five hole probe,N/m^2 j=1,2,3,4 or 5,represents ports on the probe(see figure 3)
P_{ave}	Average of indicated static pressures from ports j=2 to 5,$=\sum_{j=2}^{5} P(j)/4$,N/m^2
α	Actual angle of incidence,deg
α_i	Indicated pitch angle of probe to the freestream, $\frac{P(3)-P(5)}{q_i}$
β	Actual angle of yaw,deg
β_i	Indicated yaw angle of probe to the freestream, $=\frac{P(4)-P(2)}{q_i}$
γ	Ratio of specific heats,= 1.4 for air
q_i	Indicated dynamic pressure,$P(1)-P_{ave}$, N/m^2
s	Indicated Mach number, $=\sqrt{5\left[\left(\frac{P(1)}{P_{ave}}\right)^{1/3.5}-1\right]}$
$\vec{V}$	Velocity vector,(u,v,w),m/sec
A_k,A_{ik}	Constants used in Spline curve fit expression,k=0,1,2........,
B_k,B_{ik}	Constants defined in Spline curve fit, k=0,1,2...........
F	Defined as $\frac{H-P(1)}{H-P_{ave}}$
H	Total pressure at the probe,N/m^2

ρ_l Local density derived from five hole probe, kg/m^3

u_l Local velocity, m/sec

p_{T_l} Local total pressure, $= H$ for $M_l < 1$

$$= H \left[\frac{7M_l^2 - 1}{6}\right]^{2.5} * \left[\frac{6M_l^2}{M_l^2 + 5}\right]^{-3.5} \quad \text{for } M_l > 1$$

Subscripts and superscripts.

∞ Freestream condition

$\sim$ Root mean square value of the parameter under consideration

$-$ Steady state value of the parameter under consideration

l Local conditions

SUMMARY

An experimental investigation was carried out in connection with Aero-Optics series of tests in the 14 x 14 ft Ames transonic wind-tunnel at Moffett Field, California on the Air Force Weapons Laboratory's (AFWL) turret model. The aerodynamic parameters measured were steady and unsteady pressures (static and total fluid pressures), local mean velocities and local mean densities at selected locations along the optical beam path for the azimuth look angles of 90, 120 and 150 degrees from the turret. Two different instrumentations appropriate for obtaining steady or unsteady fluid parameter measurements are presented.

The test stream Mach numbers considered are 0.55, 0.65 and 0.75,and the Reynolds number per meter is in the range of 10^7. The results indicate that severe optical degradation can be expected at aft look azimuth angles, this degradation in optical performance increases as the azimuth angle is increased. The ratio of rms static pressure to the local mean static pressure peaks in the range of 0.07 to 0.12, and the ratio of rms total pressure to the local mean total pressure peaks in the range of 0.02 to 0.04. These values depend on the Mach number and the aft look azimuth angle. The scale lengths obtained from correlation considerations are also presented.

INTRODUCTION

The performance of an airborne optical system for astronomical research or a laser system for tracking and pointing of moving targets, is critically dependent on the variations of the refractive index in the aerodynamic medium which these electromagnetic waves have to traverse. Since the index of refraction is directly related to the density field of the medium through the Gladstone-Dale relationship, and since there is no known density monitoring instrument presently available, the required data on the density field have to be indirectly derived from a combination of theoretical considerations and measured aerodynamic parameters like mass flux, static and total pressures and temperatures, both mean and root-mean-square values of the fluctuations.

For a number of years NASA, Ames Research Center, Moffett Field, CA and Air Force Weapons Laboratory at Kirtland Air Force Base, NM have been engaged in a cooperative venture of experimental investigations leading to both qualitative observations and quantitative measurements of various fluid parameters surrounding scaled turret models in a wind-tunnel environment. In the "*Proceedings of the Aero-Optics Symposium on Electromagnetic Wave Propagation from Aircraft*" (Ref. 1) the cumulative efforts of several investigators from past years up to Aero Optics IV tests are presented and discussed.

The present report will be concerned with a 0.30 scale " on-gimbal" turret model with a circular aperture. The aperture is surrounded by a porous projected fence. The entire turret model is mounted on a splitter plate in the wind-tunnel test section as sketched in Figure 1. The range of Mach numbers and the Reynolds numbers considered in these tests are comparable to the actual flight environment. The methods of obtaining mass flux measurements using constant temperature hot wire anemometry, and unsteady pressure (static and total pressures) parameters using a specially designed probe, are discussed by individual investigators Rose and Raman respectively in their articles in reference 1. A good overall review of wind-tunnel tests is given by Buell in reference 1. These methods will not be discussed in the present paper, nor will we go into the calculation of rms density value using measured mass flux, pressure and temperature along with all the necessary assumptions in such a manipulation. Such a discussion is given by Rose in another article in reference 1.

The new five hole conical probe used in these investigations to obtain mean local Mach numbers (or velocities), local mean total and static pressures, and local mean densities in the near and wake field region of the turret will be discussed. The cone probe requires an extensive calibration procedure in a known flow field to obtain all necessary calibration data.

The correlation coefficients were obtained using two identical pressure probes with known separation distance between them. From these correlation data the scale lengths along the look azimuth direction of parameters under consideration will be derived.

EXPERIMENTAL FACILITY AND MODEL

The wind-tunnel test facility used for these investigations was the 14 x 14 ft Ames transonic wind-tunnel. A large 0.3 scale model of the Air Force "on-gimbal" turret was installed on a vertical splitter plate to avoid the unknown wind-tunnel sidewall boundary layer effects on the measurements. A sketch of the experimental set-up is given in figure 1. The tests covered the following test stream range:

$$0.55 \leq \text{free stream Mach number, } M_\infty \leq 0.75$$

$$9\times10^6 \leq \text{Reynolds number/meter, Re/m} \leq 12\times10^6$$

$$1.6\times10^4 \leq \text{dynamic pressure, q, N/m}^2 \leq 3.25\times10^4$$

Figure 1 shows the locations of five surface mounted transducers, P100 to P104, for obtaining the dynamic static pressure data. The azimuth look angle with origin at the center of the turret is shown in dashed lines for 90, 120 and 150 degrees.

These tests were carried out for zero elevation of the turret, that is, the axis of the optical path emanating from the turret along 90, 120 and 150 degrees were all parallel to the plane of the splitter plate. The turret diameter is 42.7 cm and the aperture diameter is 18 cm.

INSTRUMENTATION

The measurement of steady and unsteady pressure using a special multi-probe was discussed in detail by Raman in ~~an article in~~ reference 1. Through the use of two identical multi-probes mounted on a traverse mechanism designed by P.McQuade of the Air Force,correlation measurements were made. Mean fluid parameter measurements were made along the optical path axis for 90, 120 and 150 degrees with a specially designed conical five hole probe.

In addition Rose used hot-wire anemometry to obtain mass flux measurements, the details and results are discussed in reference 2. Both pressure and mass flux measurements are required to extract information about the density field in the near field and in the wake of the turret. The article by Rose in reference 1 gives the details about the assumptions made for the calculations and the results. Similar calculations are made using the data from the present tests.

Local steady state flow parameters in the freestream, in the shear layer region or in the disturbed flow region behind the wake of the turret model were measured with a conical tip five hole probe. The probe was specially designed, and was machined and fabricated at NASA, Ames Research Center after an extensive study of available literature on five hole probes (Ref.3,4,5 and 6).

The probe tip and the holder are sketched in figure 2. All dimensions are in millimeter units. The probe itself was tested at the US Air Force Academy 1 x 1 ft trisonic blowdown wind-tunnel facility at Colorado Springs, CO to obtain the necessary calibration data. The range of Mach numbers for these tests were $0.2 \leq M_\infty \leq 1.8$, achieved by installation of appropriate interchangeable nozzle blocks during the tests. The data obtained were analyzed to establish the required calibration curves and analytic expressions prior to the use of the probe in the 6 x 6 ft wind-tunnel tests.

The conical tip probe probe provides five pressures, $P(j)$, $j=1,2...5$ corresponding to the number of ports as shown in figure 3. The body fixed coordinate system used is also given along with the derivable expressions for u,v,w, the velocity components of velocity vector $\hat{V}$,(Ref.5). Velocities are considered in terms of Mach numbers M and later converted by multiplying by the speed of sound.

During the calibration tests the tunnel static pressure, total pressure, total temperature and the Mach number in the test section are known and the conical tip probe is tested where the angular orientation, θ and ϕ (see figure 3), is varied and the corresponding pressure $P(j)$ measured. From the known θ and ϕ the corresponding β and α angles can be determined. That is

$$\beta = \sin^{-1} (\sin \theta \sin \phi)$$

$$\alpha = \sin^{-1} (\sin \theta \cos \phi / \cos \beta)$$

Also, we define the indicated pitch angle, α_i , and the indicated yaw angle, β_i, using the measured pressures $P(j)$, $j=1,2...5$ as given below

$$P_{ave} = \sum_{j=2}^{5} P(j)/4$$

$$\alpha_i = \frac{P(3) - P(5)}{P(1) - P_{ave}}$$

$$\beta_i = \frac{P(4) - P(2)}{P(1) - P_{ave}}$$

The indicated angles α_i and β_i are plotted against the actual angle of incidence, α, and the actual yaw angle, β , respectively, and from these the relationships between α , α_i , β and β_i are established as

$$\alpha = 40 \tanh (0.52\ \alpha_I)$$

$$\beta = 40 \tanh (0.52\ \beta_I)$$

Thus we are in a position to calculate the direction the velocity vector $\hat{V}$ makes with the probe axis.

Now let us define the indicated Mach number, S, as

$$S = \left\{ \left[\left(\frac{P(1)}{P_{ave}} \right)^{2/7} - 1 \right] * 5 \right\}^{1/2}$$

This Mach number, S, is compared with the local test section Mach number M_l for each pitch angle, θ . Through the use of a spline curve fit program the analytic relationship of parameters S and M_l is established. The expression thus obtained is

$$M_l = A_o + (1 + A_1)S + \sum_{k=2}^{k=18} A_k\ (B_k - S)^2 \ln\ (B_k - S)^2$$

where A_k are functions of θ and B_k are constants. The values of A_k and B_k are given below. The angle of θ is the actual angle of attitude between the freestream velocity vector and the probe axis and is given as

$$\theta = \tan^{-1} (\sin^2 \alpha + \tan^2 \beta)^{\frac{1}{2}} / \cos \alpha$$

in degrees. Since we have obtained M_l , α and β so far, the velocity and its components can be resolved completely from the five hole probe pressure data.

$$A_0 = -1.4819\ E-1 + 3.5379\ E-3 * \theta - 3.0825\ E-4 * \theta^2 + 6.0700\ E-6 * \theta^3$$

$$A_1 = 8.2572\ E-1 - 1.1320\ E-2 * \theta + 4.9288\ E-4 * \theta^2 - 5.3700\ E-6 * \theta^3$$

$$A_2 = 2.8175\ E-1 - 1.0063\ E-2 * \theta + 8.2650\ E-4 * \theta^2 - 1.9790\ E-5 * \theta^3 \ ; \ B_2 = 0$$

$$A_3 = -1.4089\ E-1 + 1.4581\ E-2 * \theta - 1.3534\ E-3 * \theta^2 + 2.9750\ E-5 * \theta^3 \ ; \ B_3 = 0.10$$

$$A_4 = 1.3524\ E-2 - 4.0738\ E-3 * \theta + 4.5063\ E-4 * \theta^2 - 1.1110\ E-5 * \theta^3 \ ; \ B_4 = 0.20$$

$$A_5 = 4.0656\ E-2 - 9.9740\ E-3 * \theta + 5.4800\ E-4 * \theta^2 - 8.0300\ E-6 * \theta^3 \ ; \ B_5 = 0.30$$

$$A_6 = -7.5889\ E-3 + 1.8894\ E-2 * \theta - 1.0980\ E-3 * \theta^2 + 1.7610\ E-5 * \theta^3 \ ; \ B_6 = 0.35$$

$$A_7 = 5.3912\ E-2 - 1.9800\ E-2 * \theta + 5.5526\ E-4 * \theta^2 + 3.1100\ E-6 * \theta^3 \ ; \ B_7 = 0.40$$

$$A_8 = 2.8045\ E-2 + 1.0988\ E-2 * \theta + 5.8053\ E-4 * \theta^2 - 2.2710\ E-5 * \theta^3 \ ; \ B_8 = 0.46$$

$$A_9 = 3.0197\ E-1 - 2.8066\ E-2 * \theta - 1.9680\ E-4 * \theta^2 + 2.4390\ E-5 * \theta^3 \ ; \ B_9 = 0.53$$

$$A_{10} = 2.6355\ E-1 + 2.1494\ E-2 * \theta + 1.7337\ E-3 * \theta^2 - 7.3770\ E-5 * \theta^3 \ ; \ B_{10} = 0.60$$

$$A_{11} = 2.3345 - 7.4889\ E-2 * \theta - 1.1174\ E-2 * \theta^2 + 3.8750\ E-4 * \theta^3 \ ; \ B_{11} = 0.63$$

$$A_{12} = -7.6371 + 8.9829\ E-1 * \theta + 1.9324\ E-2 * \theta^2 - 1.4235\ E-3 * \theta^3 \ ; \ B_{12} = 0.67$$

$$A_{13} = -4.3933 - 2.5285 * \theta + 2.7040\ E-2 * \theta^2 + 1.8331\ E-3 * \theta^3 \ ; \ B_{13} = 0.70$$

$$A_{14} = 7.0889 + 2.6634 * \theta - 9.6695\ E-2 * \theta^2 + 2.6420\ E-4 * \theta^3 \ ; \ B_{14} = 0.72$$

$$A_{15} = 2.9364 - 1.3786 * \theta + 9.3050\ E-2 * \theta^2 - 1.7324\ E-3 * \theta^3 \ ; \ B_{15} = 0.75$$

$$A_{16} = -1.2053 + 4.1122\ E-1 * \theta - 2.8499\ E-2 * \theta^2 + 5.9386\ E-4 * \theta^3 \ ; \ B_{16} = 0.79$$

$$A_{17} = 3.0879\ E-1 + 9.8343\ E-2 * \theta - 1.5733\ E-2 * \theta^2 + 3.7172\ E-4 * \theta^3 \ ; \ B_{17} = 0.86$$

$$A_{18} = -2.6767\ E-1 - 8.2292\ E-2 * \theta + 1.0544\ E-2 * \theta^2 - 2.3189\ E-4 * \theta^3 \ ; \ B_{18} = 0.93$$

In order to obtain a relationship between local total pressure P_{T_l} and measured P(j) we define F as

$$F = \frac{H - P(1)}{H - P_{ave}}$$

where H is the total pressure at the probe location. For subsonic flow $M_l < 1$, $H = P_{T_l}$. But in supersonic flow situations a standing bow shock wave would exist ahead of the conical probe, and H then represents the total pressure behind the bow shock wave. This is the value of H expressed as

$$H = P_{T_l} \left(\frac{6M_l^2}{M_l^2 + 5}\right)^{3.5} \cdot \left(\frac{7M_l^2 - 1}{6}\right)^{-2.5} \quad \text{for} \quad M_l > 1$$

By considering F and obtaining an expression for F as a function of θ and M_l from our calibration tests, we are in a position to obtain the total pressure H in an unknown flow field from measurements of P(j) and an expression for F. Once H is known, the local total pressure in the flow, that is, ahead of the bow shock wave of the probe, can be established by rewriting for

$$P_{T_l} = H \left[\frac{7M_l^2 - 1}{6}\right]^{2.5} \cdot \left[\frac{6M_l^2}{M_l^2 + 5}\right]^{-3.5}$$

Thus we can obtain the actual total pressure from the conical five hole probe measurements. The expression for F is given below and is a function of M_l and θ.

$$\begin{aligned} F = & (1.6004E\text{-}3*M_l + 4.5334E\text{-}4*M_l^2 - 7.6139E\text{-}4*M_l^3) \\ & + (-3.7823E\text{-}2*M_l + 4.6857E\text{-}2*M_l^2 - 1.7022E\text{-}2*M_l^3)\theta \\ & + (2.6922E\text{-}3*M_l - 2.3993E\text{-}3*M_l^2 + 6.5168E\text{-}4*M_l^3)\theta^2 \\ & + (-8.5000E\text{-}7*M_l - 1.7070E\text{-}5*M_l^2 + 9.8200E\text{-}6*M_l^3)\theta^3 \end{aligned}$$

So far the data from the five hole probe and manipulation of the data have yielded α , β , θ , M_l through spline fit curve expressions using A_K, B_K and S and the total pressure p_{T_l} using expression $F(M_l, \theta)$. Now, if we assume an adiabatic process and that the wind-tunnel total temperature, T_{T_∞} , is available, then we can obtain local mean static pressure, p_l , local mean density, ρ_l , and local mean velocity, u_l , by using the expressions

$$p_l = p_{T_l} \left(1 + M_l^2 / 5 \right)^{-3.5}$$

$$\rho_l = \frac{p_{T_l}}{286.86 \, T_{T_\infty} \left(1 + M_l^2 / 5 \right)^{2.5}}$$

$$u_l = 20.04 \, M_l \left(\frac{T_{T_\infty}}{1 + M_l^2 / 5} \right)^{\frac{1}{2}}$$

since $\gamma = 1.4$ for air.

TESTS

The tests carried out involved several model changes in orientation of turret look angles θ. The instrumentation changes involved changing the five hole probe or multi-probes on the appropriate probe holders provided on the traverse mechanism and routing all instrument cables to the signal conditioning and data acquisition station. All standard calibration procedures for all instruments prior to each set of tests, were adhered to, and some on-line data processing and observation of results as the tests progressed were possible through effective use of desktop calculators, plotters and oscilloscopes.

RESULTS AND DISCUSSION

Steady State Measurements

The mean local measurements of fluid flow parameters, namely, the local Mach number, M_l , the local total pressure, p_{Tl}, and the local density, ρ_l , along the radial axis of the optical path for azimuth angles 90, 120 and 150 degrees are presented in nondimensional form of M_l / M_∞ , $p_{Tl} / p_{T\infty}$ and ρ_l / ρ_∞ in figures 4, 5 and 6. These measurements were used to obtain an analytic expression for M_l / M_∞ , $(= Y_1)$; $p_{Tl}/p_{T\infty}$, $(= Y_2)$ and ρ_l / ρ_∞ $(= Y_3)$ through the spline curve fit procedure and yielded data for the solid curve shown through the data points in figures 4, 5, 6. The constants A_k and B_k entering in the spline expressions

$$Y_i(R) = A_{io} + A_{i1} R + \sum_{k=2} A_{ik}(B_{ik} - R)^2 \ln (B_{ik} - R)^2$$

where $i = 1, 2$ or 3 to yield values for $Y_1(R)$,$Y_2(R)$ or $Y_3(R)$,are given in tables 1, 2 and 3. A note of caution is necessary when using the above expression for calculations: always select $R \neq B_{ik}$ values. The analytic expressions for Y_1, Y_2 and Y_3 were useful for normalization of unsteady flow parameter data to their respective local mean parameters. These are presented later in this report.

From the data in figures 4, 5 and 6 one is able to obtain the magnitude of the shear layer and the gradients of M_l and ρ_l . These are given in table 4. One can even obtain the pressure gradients from figures 4, 5 and 6. The shear layer is thin and the gradients of M_l and ρ_l are large for an azimuth angle of 90 degrees. As the azimuth angle is increased, the shear layer thickness increases and the magnitude of the local density gradients decreases for a given Mach number. Also, for a given θ , the local Mach number gradients increase with an increase in Mach number. The increase in shear layer defines the optical path length, L, variations as a function of θ . Along this path the optics performance characteristics degrade through the shear layer turbulence.

Dynamic Measurements

In figures 7 and 8 the unsteady static and total pressure measurements obtained by the combination probe are presented in normalized quantities. The appropriate local mean static or total pressures are used as the normalizing pressures of the unsteady data presented. The peak unsteady static pressures fall in the range of 7 to 12 % of their local mean pressures for both θ = 120 and θ = 150 and for all Mach numbers. Some of these unexpectedly high values of unsteady static pressures may be due to variations in the local stream direction as it approaches the static pressure port. Only through simultaneous flow visualization during the static pressure measurements can this reasonable conjecture be substantiated. The maximum unsteady total pressure data fall within 4 % of its local mean pressure for all Mach numbers and azimuth angles.

The correlation function measurements of the unsteady pressures for various Mach numbers and azimuth angles were carried out using two identical multiprobes (details of the probe are described in the article by Raman in reference 1), varying the separation distance between these two probes. In figure 9 the cross correlation function for an azimuth angle of 120 degrees and for Mach numbers 0.55, 0.65 and 0.75 is presented for various separation distances while one probe was held at the radial location, R = 28cm. In figure 10 similar data are presented for θ = 150 and R = 30cm. In both figures

9 and 10 the static and total pressures were considered. In table 5 the scale lengths obtained from several of these correlation measurements are presented for R = 30 cm for different Mach numbers.

For an azimuth angle of 120 degrees and radial location around 30 cm the scale lengths are smaller in magnitude than for the azimuth angle of 150 degrees and R = 30 cm for both static and total pressures presented here. An examination of figures 5 and 6 indicates the different regions that are being explored in these measurements. When θ = 120 degrees and R = 30 cm, the initial start of the shear layer region is considered, while for θ = 150 degrees and R = 30 cm the wake region is examined. This difference in regions explored could account for the large differences in scale lengths observed in the data presented in table 5.

In figures 11 and 12 the cross correlation functions are presented for a fixed separation distance between the probes as a function of radial location, R. These figures shed some light on the decay of the pressure signature observed in the explored regions. The decay rate in the shear region (figure 11) is much greater than that observed for the wake region (figure 12). Please note the scale differences in abscissa in figures 11 and 12.

CONCLUSIONS

From the results of the present experimental investigation on the turret model in the 14 x 14 ft transonic wind-tunnel at Ames Research Center, the following conclusions can be made:

1) The five hole conical probe, once completely calibrated, can be successfully deployed to yield information on mean flow parameters in an unknown flow. This instrument gives local Mach number, the direction of flow and the total pressure. From these values and the adiabatic assumption all other flow parameters can be derived.

2) The unsteady pressures and correlations can be measured using the multi-probes. The maximum of RMS static pressure occurs around the radial distance of R = 31 cm for an azimuth angle of 120^o, this is the region where maximum pressure gradients occur, see figure 5 (a,b,c). The same conclusions can be drawn for the azimuth angle of 150^o and a radial distance of around 46 cm.

3) The scale lengths obtained from the correlation measurements of static pressures are around 3 cm in the shear layer region for an azimuth angle of 120^o and seem to be dependent on Mach number M_∞. In the wake region with an azimuth angle of 150^o the scale lengths vary from 8 - 15 cm and seem to depend on Mach number M_∞.

4) One obtains an understanding of the relative decay of turbulence by examining figures 11 and 12. The decay rate seems to be more pronounced in the shear layer (figure 11) than in the wake region (figure 12) when one examines the peak correlations for a given separation distance as they progress along the radial path. Note that the saparation distance in figure 11 is ΔP = 0.5 cm while ΔP = 2 cm for figure 12. In spite of this difference the decay indi-

cated in figure 12 is slower than that in figure 11.

5) The static pressure fluctuations combined with velocity fluctuations contributes to density variations in the flow. This is pointed out in reference 2.

All the experiments carried out so far are only for zero elevation of the turret.

REFERENCES

1. *Proceedings of the Aero-Optics Symposium on Electromagnetic Wave Propagation from Aircraft.* NASA CP 2121, April 1980.

2. Rose, W.C. et al. *Nearfield Aerodynamics and Optical Propagation Characteristics of a large-scale Turret Model.* AFWL TR -162, May 1981.

3. Breyer, D.W. and Pankhurst, R.C. *Pressure Probe Methods for Determining Wind Speed and Direction.* London, Her Majesty's Stationary Office, National Physical Laboratory, 1971.

4. Chue, S.H. *Pressure Probes for Fluid Measurements.* Prog.Aerospace Sci. 1975, v.16 no.2, pp 107-122. Pergamon Press.

5. Barker, K., Gallington, R.W. and Minster, S. *Calibration of Five-Hole Probes for On-Line Data Reduction.* Aeronautics Digest - Spring 1979. USAFA-TR-79-7, USAF Academy, Colorado. July 1979.

6. Dudinski, T.J. and Krause, L.N. *Flow Direction Measurements with Fixed-Position Probes in Subsonic Flow over a Range of Reynolds Number.* NASA TMX-1904, N69 40059.

Table 1

Azimuth angle = 90

Freestream: Mach No.=0.55 Total Pressure, N/m^2 =1.01*10^5 Density, kg/m^3=0.979

k	A_{ik} i=1	A_{ik} i=2	A_{ik} i=3	B_{ik}	Measured values using five hole probe Y_1	Y_2	Y_3
0	1.880E-1	7.161E-1	8.216E-1				
1	5.104E-2	1.331E-2	5.936E-3				
2	1.772E-2	2.653E-3	3.930E-4	20.48	0.18752	0.76031	0.87848
3	-2.159E-2	2.068E-3	2.819E-3	21.79	0.20620	0.76234	0.88082
4	-3.276E-2	-6.137E-3	-3.838E-3	22.40	0.36699	0.77574	0.87989
5	-2.627E-2	-2.277E-2	-5.282E-3	23.09	0.71869	0.83711	0.89637
6	8.742E-2	2.864E-2	5.852E-3	23.72	1.06557	0.94448	0.92746
7	-2.199E-2	-3.374E-3	5.720E-4	25.00	1.11585	0.99064	0.95687
8	-1.684E-3	-8.893E-4	-4.559E-4	27.56	1.09289	0.98962	0.96354
9	-8.463E-4	-1.943E-4	-5.955E-5	35.31	1.04927	0.99180	0.97916

Freestream: Mach No.=0.65 Total Pressure, N/m^2 =1.01*10^5 Density, kg/m^3=0.928

k	A_{ik} i=1	A_{ik} i=2	A_{ik} i=3	B_{ik}	Y_1	Y_2	Y_3
0	1.610E-1	6.290E-1	7.568E-1				
1	5.505E-2	1.712E-2	7.638E-3				
2	1.788E-2	4.279E-3	1.495E-3	20.46	0.17230	0.68386	0.82954
3	-1.157E-2	-1.941E-3	-1.726E-3	21.17	0.17549	0.68061	0.82905
4	1.780E-3	3.399E-3	3.540E-3	21.74	0.22681	0.68462	0.83142
5	-4.692E-2	-6.651E-3	-5.451E-3	22.43	0.38402	0.70461	0.83428
6	-3.039E-2	-3.074E-2	-2.901E-3	23.06	0.71351	0.77753	0.85714
7	9.368E-2	3.620E-2	4.089E-3	23.69	1.07253	0.91515	0.89142
8	-2.205E-2	-3.008E-3	1.743E-3	25.03	1.12865	0.98920	0.93714
9	-1.501E-3	-1.283E-3	-7.123E-4	27.53	1.10931	0.98931	0.94571
10	-9.049E-4	-2.582E-4	-7.721E-5	35.28	1.06656	0.99096	0.96571

Freestream: Mach No.=0.75 Total Pressure, N/m^2 =1.01*10^5 Density, kg/m^3=0.825

k	A_{ik} i=1	A_{ik} i=2	A_{ik} i=3	B_{ik}	Y_1	Y_2	Y_3
0	2.826E-1	5.379E-1	6.450E-1				
1	5.459E-2	2.380E-2	1.126E-2				
2	2.190E-2	5.225E-3	1.197E-3	20.45	0.22715	0.59069	0.75937
3	-1.018E-2	-2.518E-4	1.004E-3	21.11	0.22542	0.59203	0.76131
4	-2.013E-2	4.787E-3	-5.291E-4	21.78	0.30266	0.60161	0.76323
5	-5.563E-2	-2.858E-2	-4.770E-3	22.40	0.52498	0.64060	0.77500
6	4.863E-2	-4.912E-3	-2.227E-3	23.11	0.95652	0.79576	0.81250
7	4.210E-2	3.635E-2	5.791E-3	23.91	1.22673	0.98095	0.86562
8	-2.512E-2	-1.163E-2	2.351E-4	25.03	1.17643	0.99210	0.89966
9	-6.816E-4	-6.183E-4	-5.931E-4	27.60	1.14181	0.99112	0.91509
10	-8.943E-4	-3.721E-4	-1.081E-4	35.28	1.08266	0.99077	0.94968

Table 2

Azimuth angle = 120

Freestream: Mach No.=0.55 Total Pressure, N/m^2 =1.01*10^5 Density, kg/m^3=0.979

k	A_{ik} i=1	i=2	i=3	B_{1k}	Measured values using five hole probe Y_1	Y_2	Y_3
0	-4.802E-1	5.328E-1	7.531E-3				
1	5.660E-2	1.272E-2	4.648E-3				
2	9.307E-3	1.612E-3	3.074E-4	26.67	0.16424	0.74042	0.85340
3	-2.653E-2	-2.893E-3	1.320E-4	27.94	0.21799	0.74153	0.85340
4	1.896E-2	2.305E-3	-1.890E-4	28.64	0.34545	0.75290	0.85340
5	-1.219E-2	-3.612E-3	-7.560E-4	30.48	0.62464	0.79165	0.86315
6	6.195E-3	-4.001E-5	-6.320E-4	31.75	0.91910	0.86782	0.88421
7	7.773E-3	2.933E-3	1.793E-3	33.02	1.12864	0.94584	0.91052
8	3.232E-4	7.117E-4	-1.121E-3	34.29	1.19017	0.98140	0.92105
9	-2.660E-3	-5.960E-4	6.445E-4	35.56	1.18727	0.98952	0.93386
10	3.477E-4	-9.241E-5	-4.483E-5	38.10	1.17577	0.99121	0.94179
11	-1.485E-3	-3.286E-4	-1.343E-4	40.64	1.15607	0.99140	0.94444

Freestream: Mach No.=0.65 Total Pressure, N/m^2 =1.01*10^5 Density, kg/m^3=0.928

k	i=1	i=2	i=3	B_{1k}	Y_1	Y_2	Y_3
0	-1.046	2.232E-1	6.267E-1				
1	6.642E-2	1.953E-2	6.793E-3				
2	4.260E-3	1.335E-3	4.500E-4	26.67	0.17350	0.66277	0.80571
3	-1.277E-2	-1.372E-3	-3.420E-4	29.21	0.32123	0.67315	0.80571
4	4.931E-3	-1.009E-3	-6.491E-4	30.48	0.58333	0.71624	0.81714
5	-6.162E-3	-3.992E-3	-5.641E-4	31.75	0.85758	0.79859	0.84241
6	1.440E-2	5.335E-3	1.475E-3	33.02	1.12135	0.91459	0.87356
7	-7.963E-4	8.964E-4	-8.986E-4	34.29	1.19891	0.97141	0.89142
8	-1.469E-3	-2.144E-4	9.277E-4	35.56	1.20123	0.98773	0.90857
9	-2.395E-3	-9.792E-4	-3.987E-4	38.10	1.18937	0.99020	0.91666

Freestream: Mach No.=0.75 Total Pressure, N/m^2 =1.01*10^5 Density, kg/m^3=0.825

k	i=1	i=2	i=3	B_{1k}	Y_1	Y_2	Y_3
0	-2.009E-1	3.394E-1	5.895E-1				
1	5.147E-2	1.839E-2	6.803E-3				
2	3.752E-3	1.272E-3	3.449E-4	26.67	0.15481	0.57059	0.74233
3	-6.055E-3	-1.724E-4	1.167E-4	28.79	0.25990	0.57961	0.74433
4	-2.749E-3	-1.538E-3	-1.038E-3	30.48	0.51834	0.62166	0.75390
5	-7.310E-3	-7.324E-3	-1.157E-3	31.75	0.80852	0.71488	0.78125
6	1.331E-2	7.372E-3	2.611E-3	33.02	1.13291	0.87762	0.81875
7	5.114E-3	2.129E-3	-1.270E-3	34.29	1.27200	0.96453	0.83333
8	-4.179E-3	-5.766E-4	5.693E-4	35.56	1.27285	0.98764	0.84905
9	-5.699E-4	-5.143E-4	1.450E-5	36.83	1.26133	0.99063	0.85849
10	-2.661E-4	-3.152E-4	-1.707E-4	38.10	1.24833	0.99044	0.86477
11	-7.499E-5	6.028E-5	8.742E-5	40.64	1.21814	0.99025	0.87735
12	-9.705E-4	-3.934E-4	-1.091E-4	43.18	1.20160	0.99054	0.88679

Table 3

Azimuth angle = 150

Freestream: Mach No.=0.55 Total Pressure, N/m^2 $=1.01*10^5$ Density, kg/m^3=0.979

	A_{ik}				Measured values using five hole probe		
k	i=1	i=2	i=3	B_{ik}	Y_1	Y_2	Y_3
0	-5.877E-1	4.194E-1	6.914E-1				
1	1.868E-2	5.444E-3	2.261E-3				
2	3.013E-4	3.627E-5	-5.169E-6	25.40	0.19255	0.74314	0.85677
3	-1.001E-4	1.431E-5	3.706E-5	30.48	0.17653	0.74470	0.85937
4	1.147E-4	1.015E-4	8.039E-5	35.56	0.18330	0.74041	0.85340
5	2.314E-4	-3.759E-4	-5.383E-4	40.64	0.24878	0.73893	0.84816
6	2.3[illegible]2E-3	-1.412E-3	-1.774E-3	45.72	0.56672	0.77530	0.85564
7	1.199E-3	-6.306E-4	-9.690E-4	50.80	0.92831	0.86436	0.87926
8	6.429E-4	3.582E-4	1.673E-4	55.88	1.12014	0.94177	0.90814
9	-6.216E-4	-1.328E-4	-1.174E-6	60.71	1.14363	0.97139	0.93157
10	-1.325E-3	1.341E-3	1.852E-3	48.26	0.74290	0.83621	0.89210
11	-2.754E-3	6.991E-4	1.151E-3	43.18	0.34786	0.75852	0.86315

Freestream: Mach No.=0.75 Total Pressure, N/m^2 $=10^5$ Density, kg/m^3=0.825

0	-1.608	-4.178E-1	3.514E-1				
1	2.943E-2	1.297E-2	4.328E-3				
2	2.793E-4	1.156E-4	5.117E-5	29.21	0.22096	0.56094	0.72274
3	3.241E-4	4.360E-5	3.680E-5	35.56	0.21266	0.55240	0.71076
4	-8.110E-4	-6.991E-5	-8.992E-5	40.64	0.20772	0.54397	0.70061
5	-1.244E-5	4.669E-5	1.046E-4	45.72	0.39306	0.57008	0.71296
6	-8.251E-4	-3.765E-4	-2.810E-4	48.26	0.53938	0.60287	0.72530
7	9.849E-4	5.041E-6	3.791E-5	50.80	0.72223	0.66331	0.75233
8	6.826E-5	2.835E-4	3.083E-4	53.34	0.87222	0.73524	0.78086
9	-2.227E-4	-6.648E-4	-4.838E-4	55.88	1.00467	0.80785	0.80246
10	2.148E-4	6.169E-4	3.145E-4	57.91	1.10882	0.87990	0.82972

Table 4. Shear Layer Thickness and Local Density Gradients.

	= 90			= 120			= 150	
	M = 0.55	M = 0.65	M =0.75	M =0.55	M =0.65	M =0.75	M =0.55	M =0.75
Shear Layer Thickness, cm.	4.0	5.5	6.0	9.0	10.0	9.5	18.0	18.0
dM/dR	0.120	0.150	0.230	0.160	0.170	0.185	0.040	0.050
dρ/dR	0.220	0.205	0.190	0.024	0.018	0.014	0.010	0.008

Table 5. Scale lengths Obtained from Correlation Considerations.

Static Pressures l_r, cm	M	θ degree	Total Pressures l_r, cm
2.80	0.55	120	0.62
2.82	0.65	120	1.01
2.97	0.75	120	0.42
8.28	0.55	150	2.86
9.17	0.65	150	2.18
14.50	0.75	150	5.32

ORIGINAL PAGE IS
OF POOR QUALITY

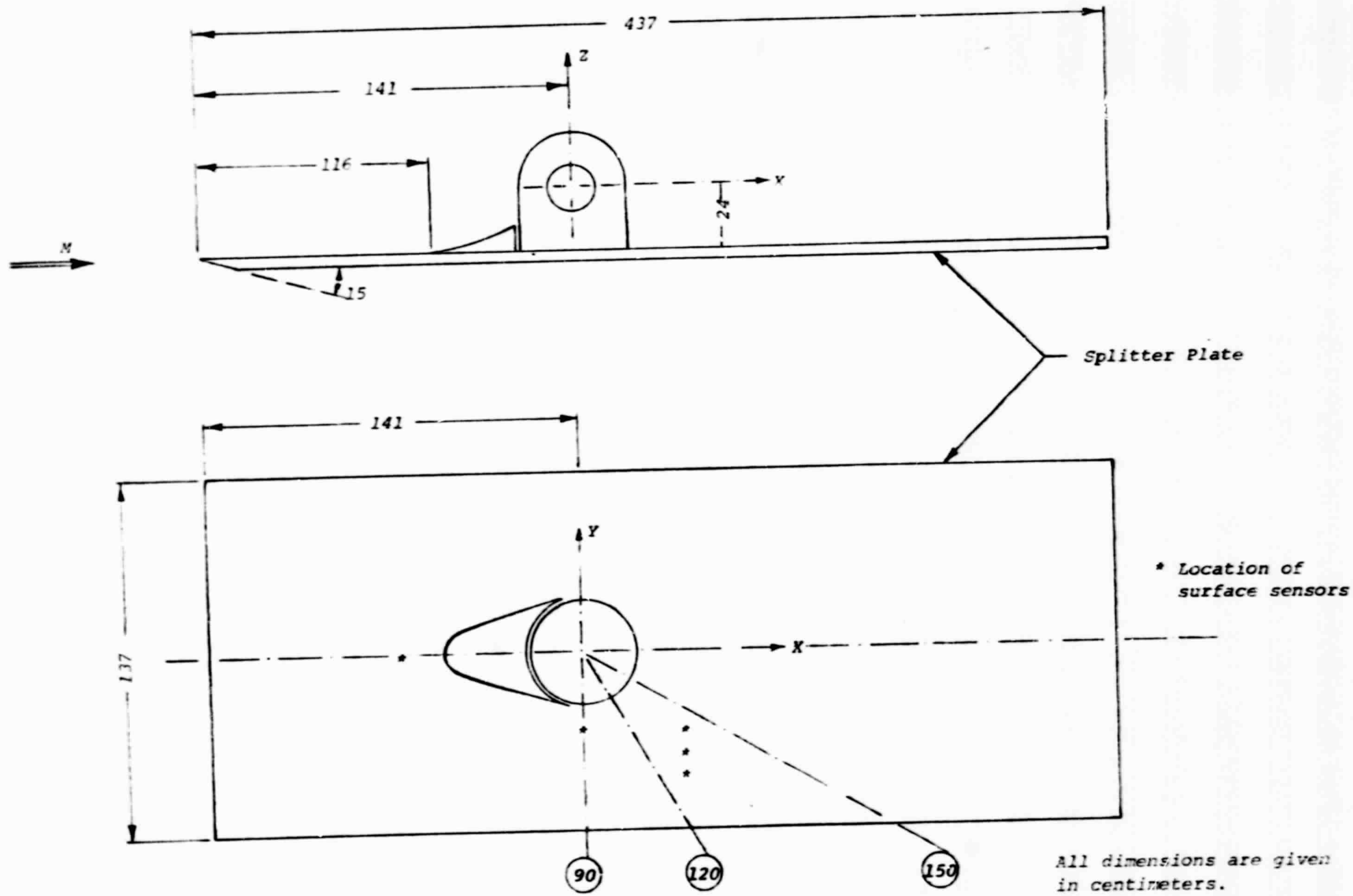

Figure 1. Sketch of turret model in the 14 x 14 ft wind-tunnel.

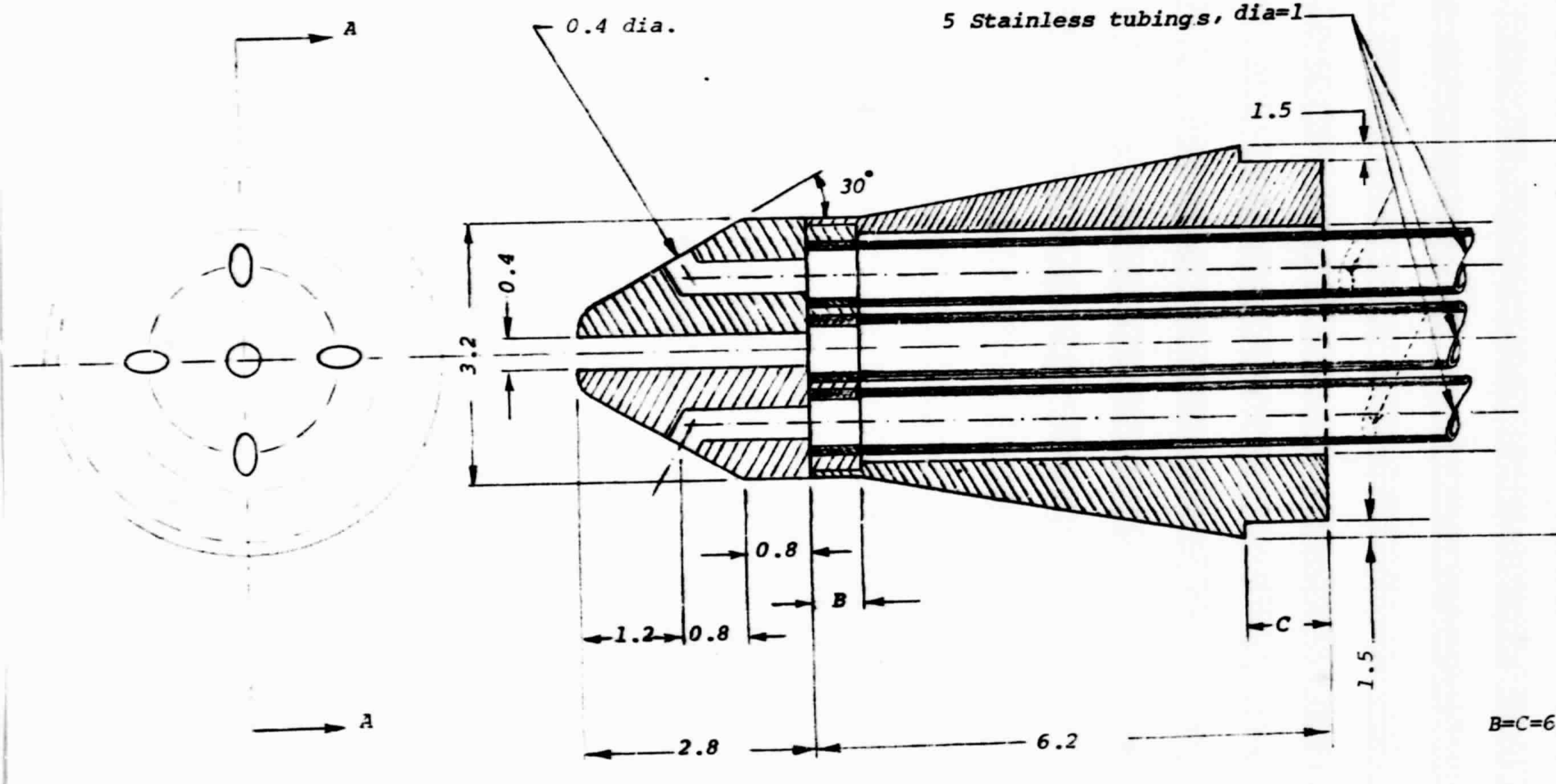

All dimensions are given in millimeters.

SECTION -- AA

Figure 2. Details of cone tip five-hole probe

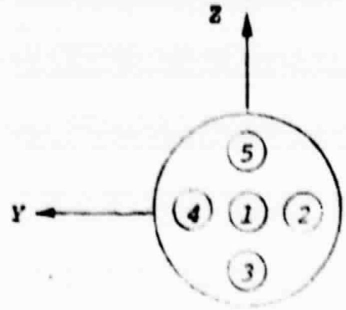

Numbering system of ports

FRONT VIEW

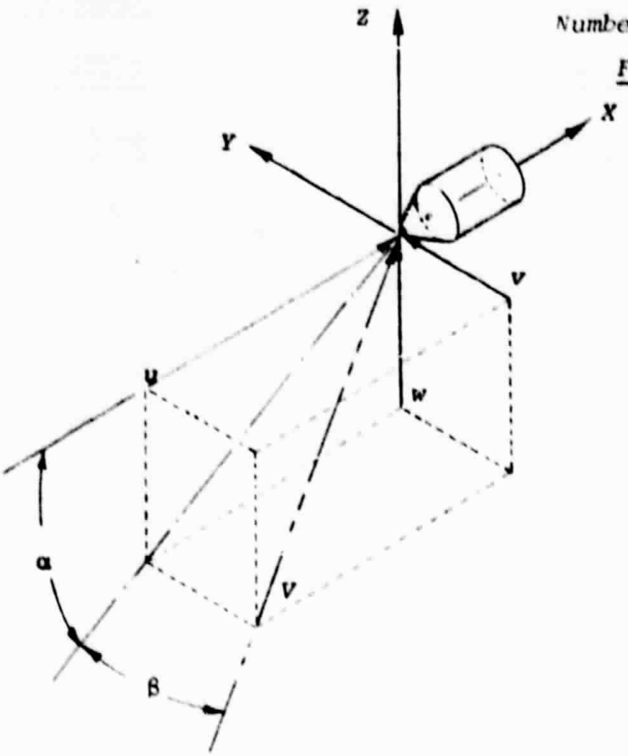

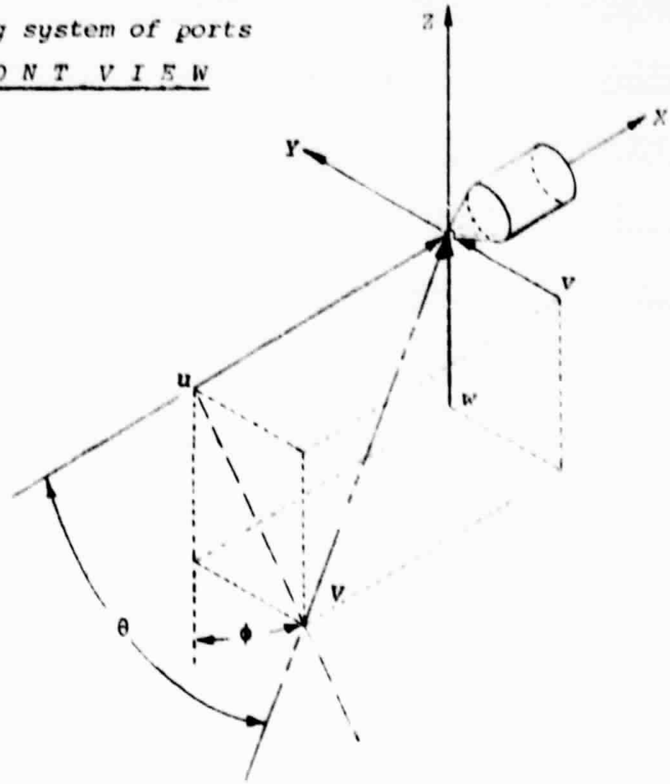

$u = V \cos\alpha \cos\beta$

$v = V \sin\beta$

$w = V \sin\alpha \cos\beta$

$u = V \cos\theta$

$v = V \sin\theta \sin\phi$

$w = V \sin\theta \cos\phi$

$\sin\alpha = \sin\theta \cos\phi / \cos\beta$

$\sin\beta = \sin\theta \sin\phi$

$\tan\theta = (\sin^2\alpha + \tan^2\beta)^{1/2} / \cos\alpha$

Figure 3. Body - Fixed Coordinate System

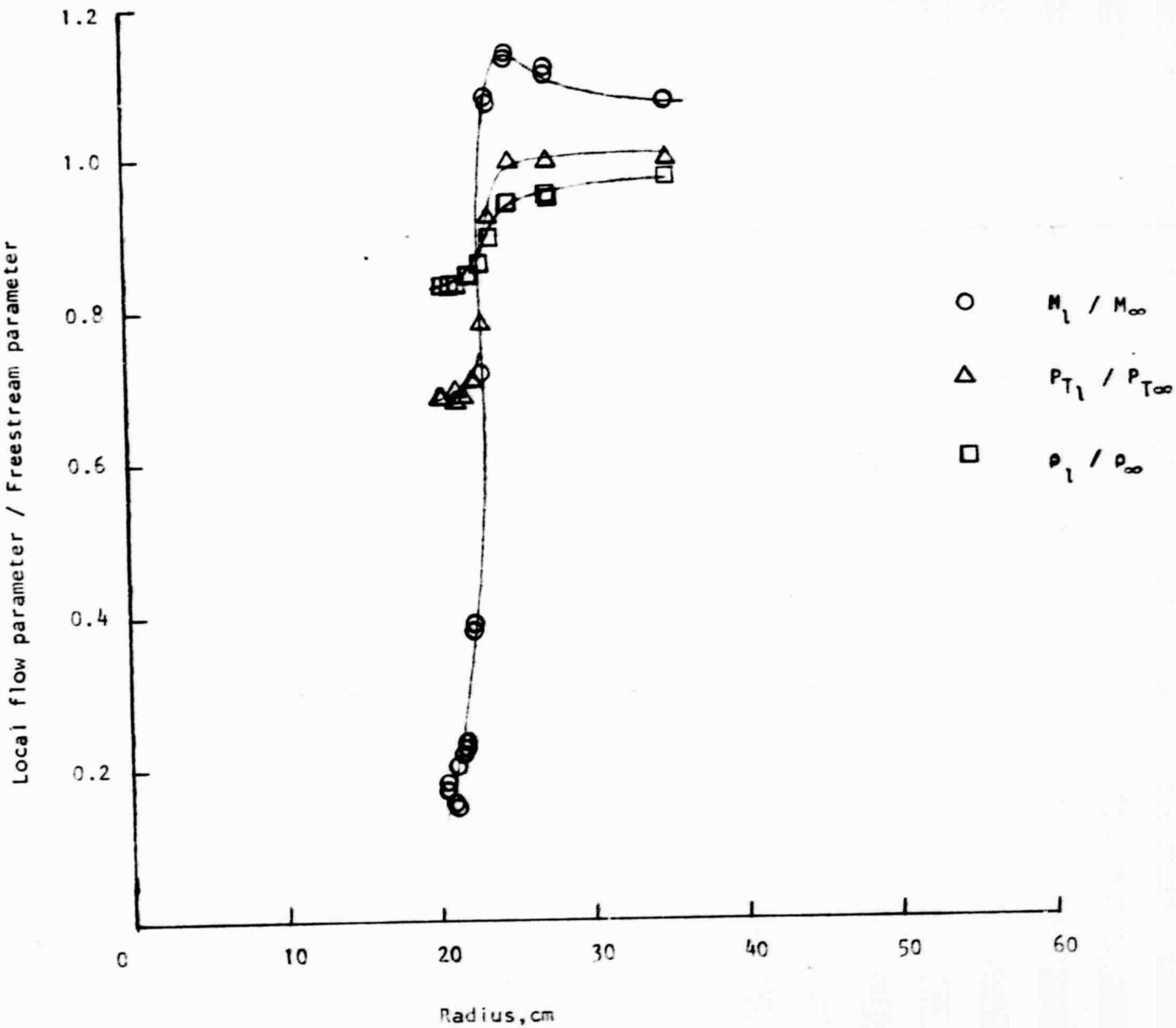

Figure 4. (a) Local Flow Parameter Distribution.

$\theta = 90^\circ \quad M_\infty = 0.55$

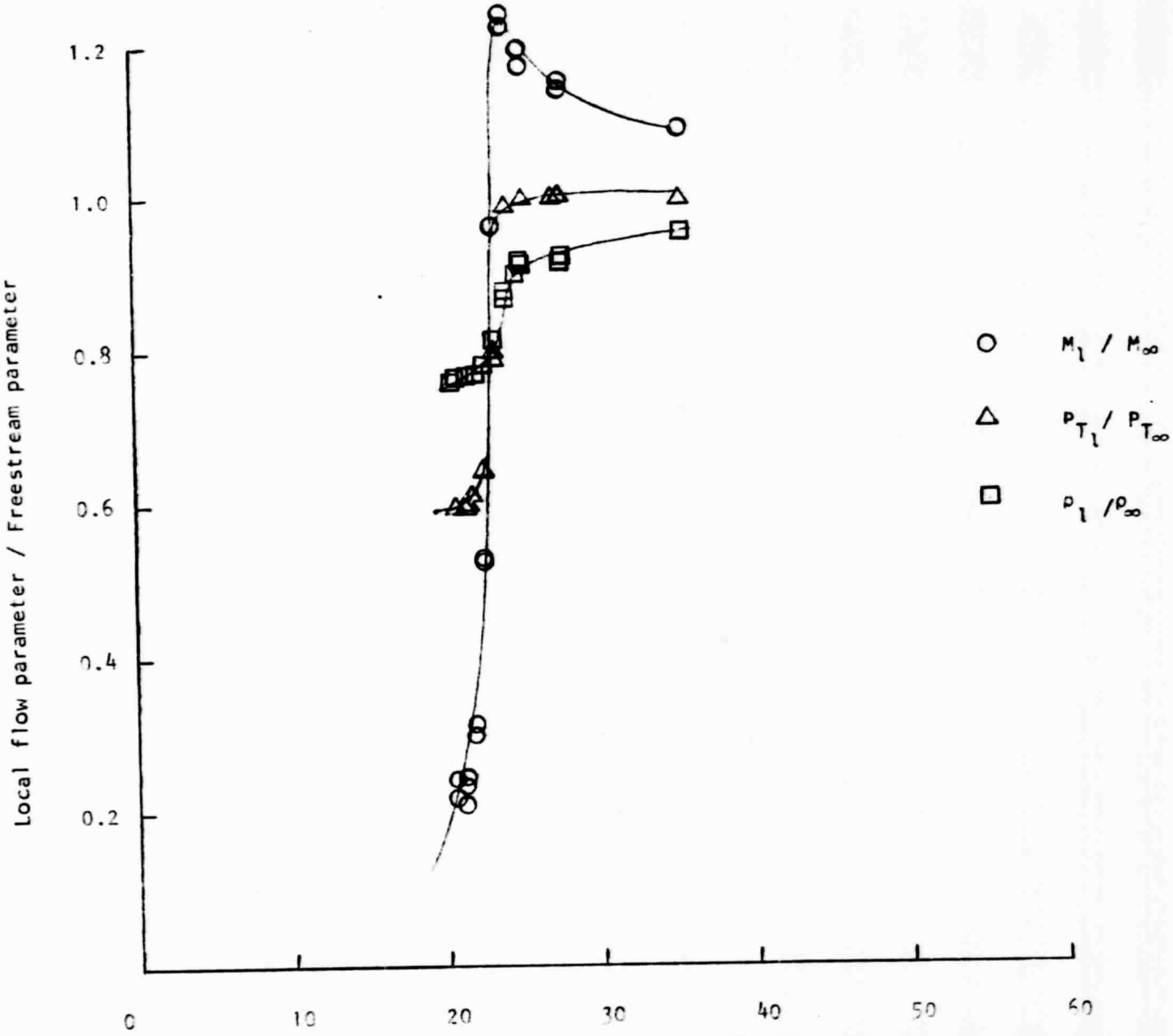

Figure 4. (b) Local Flow Parameter Distribution.
$\theta = 90°$ $M_\infty = 0.65$

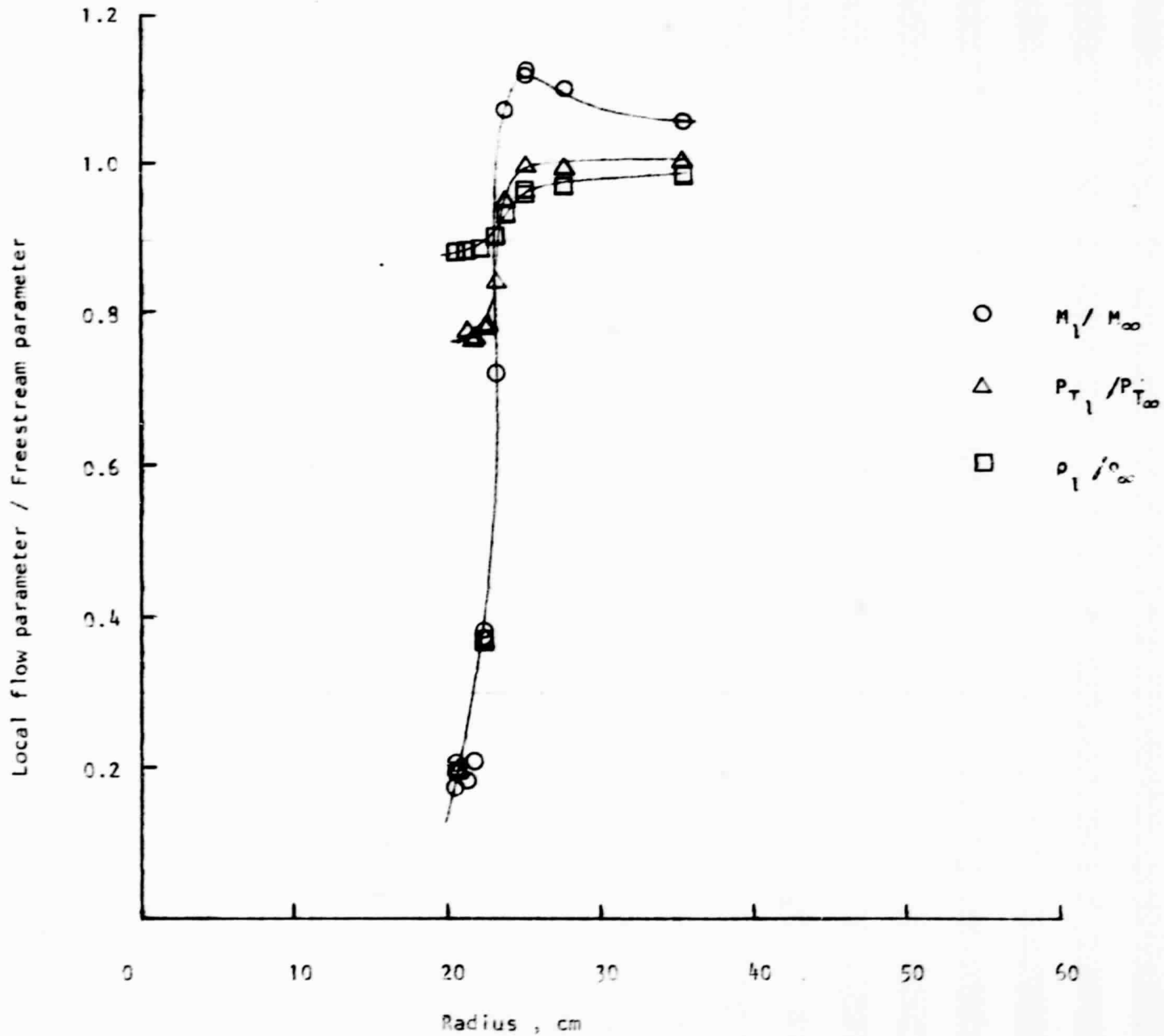

Figure 4. (c) Local Flow Parameter Distribution.
$\theta = 90^o \quad M_\infty = 0.75$

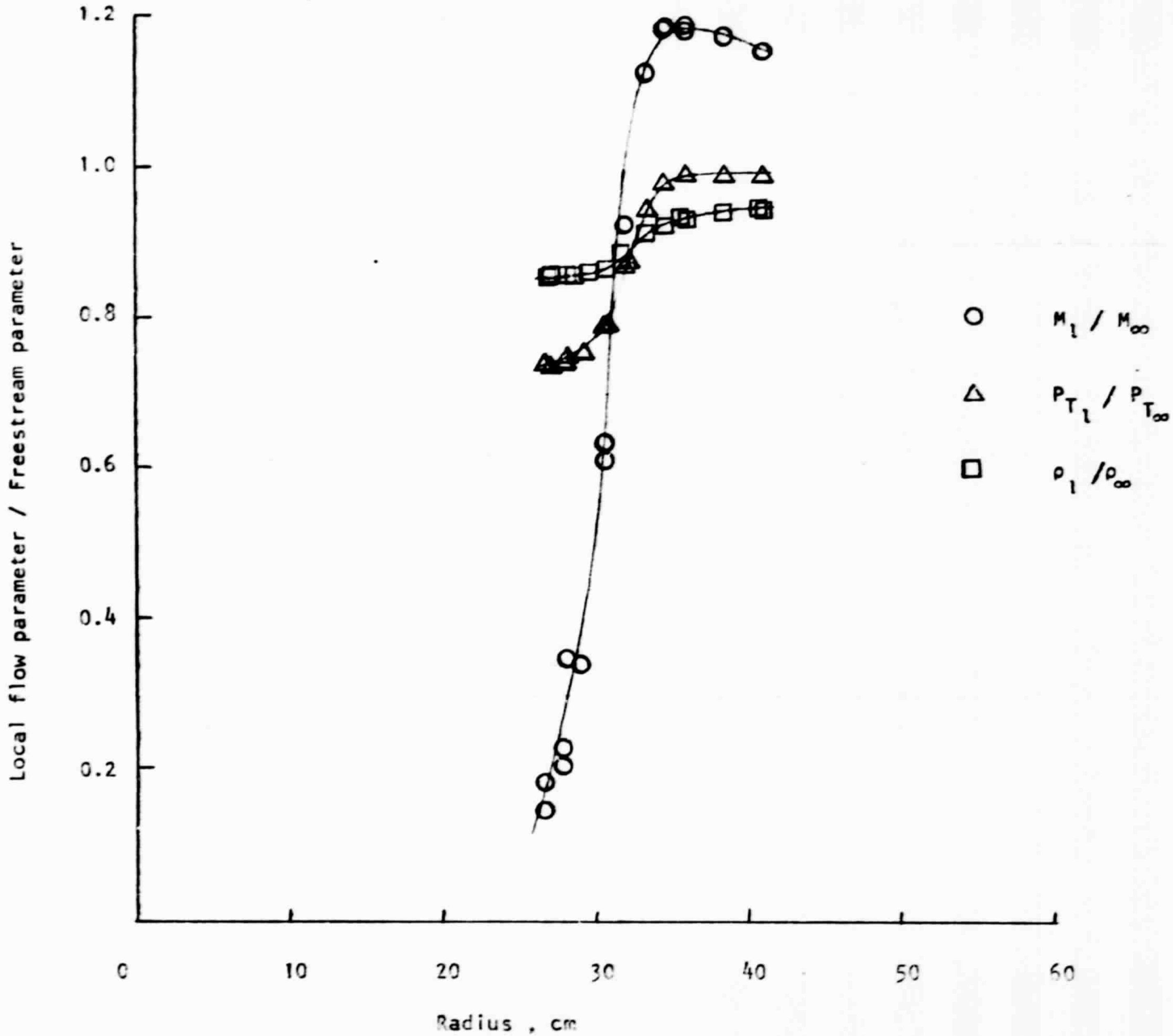

Figure 5. (a) Local Flow Parameter Distribution.

$\theta = 120^o \quad M_\infty = 0.55$

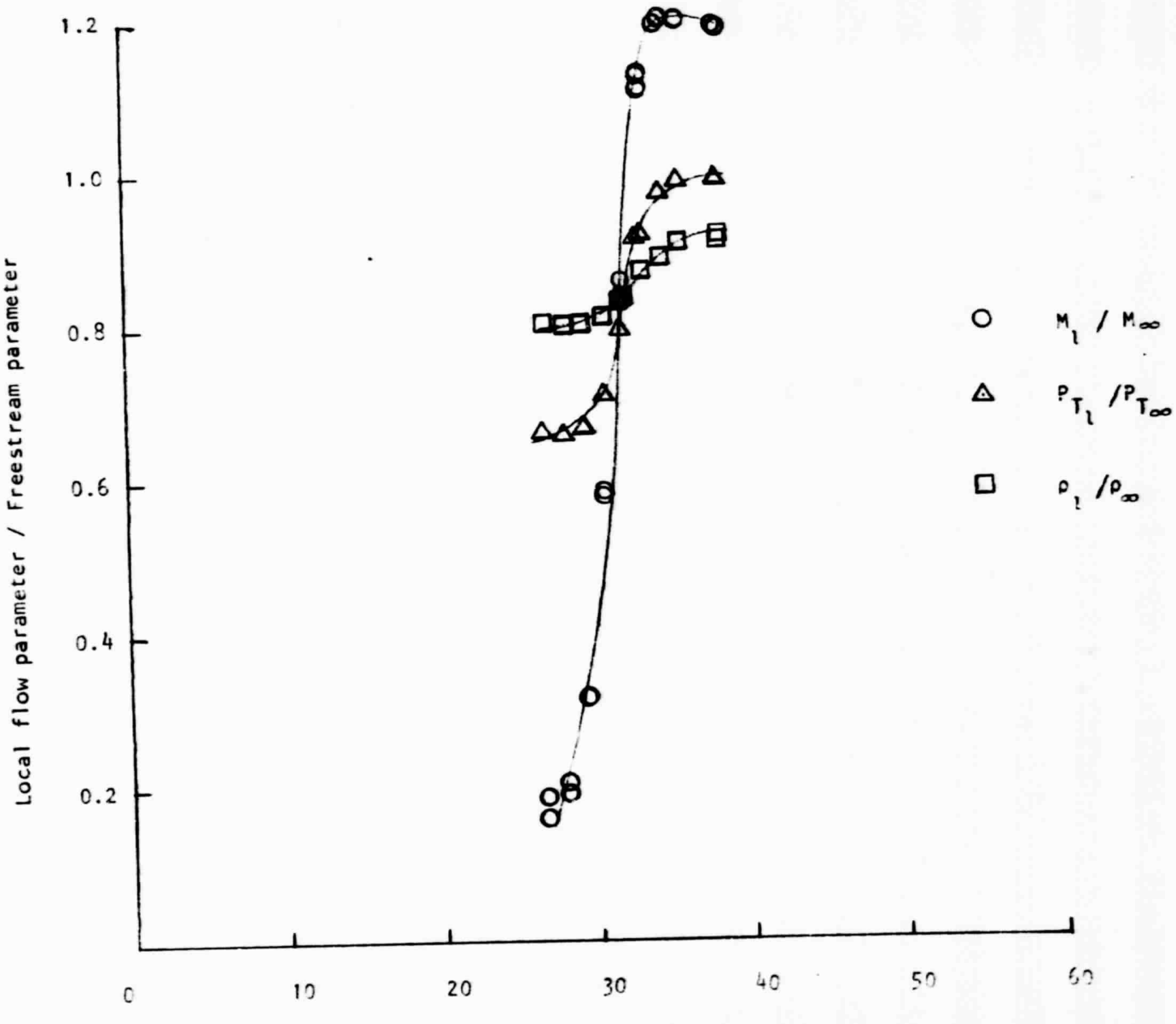

Figure 5. (b) Local Flow Parameter Distribution.
$\theta = 120^\circ$ $M_\infty = 0.65$

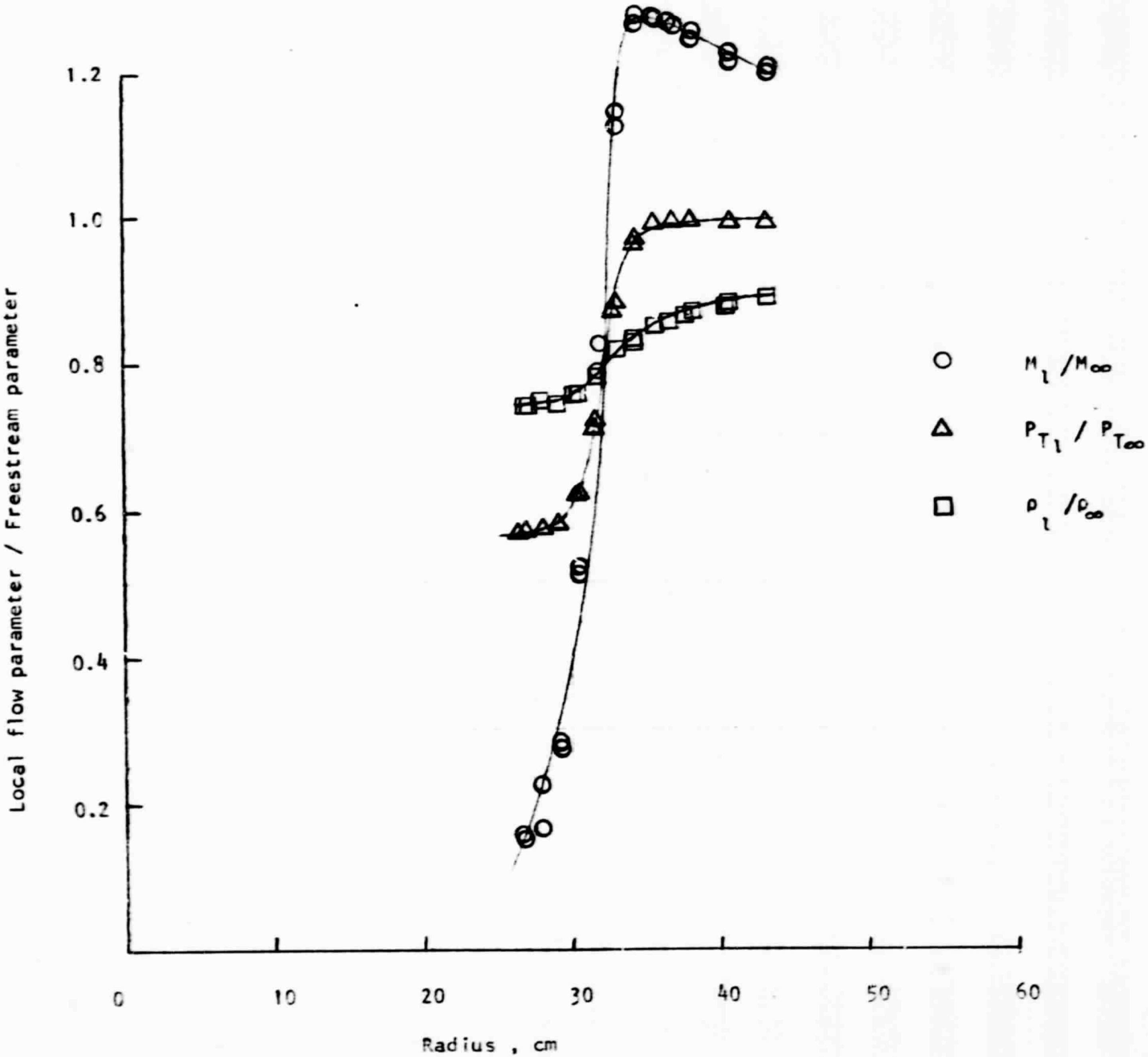

Figure 5. (c) Local Flow Parameter Distribution
$\theta = 120^0 \quad M_\infty = 0.75$

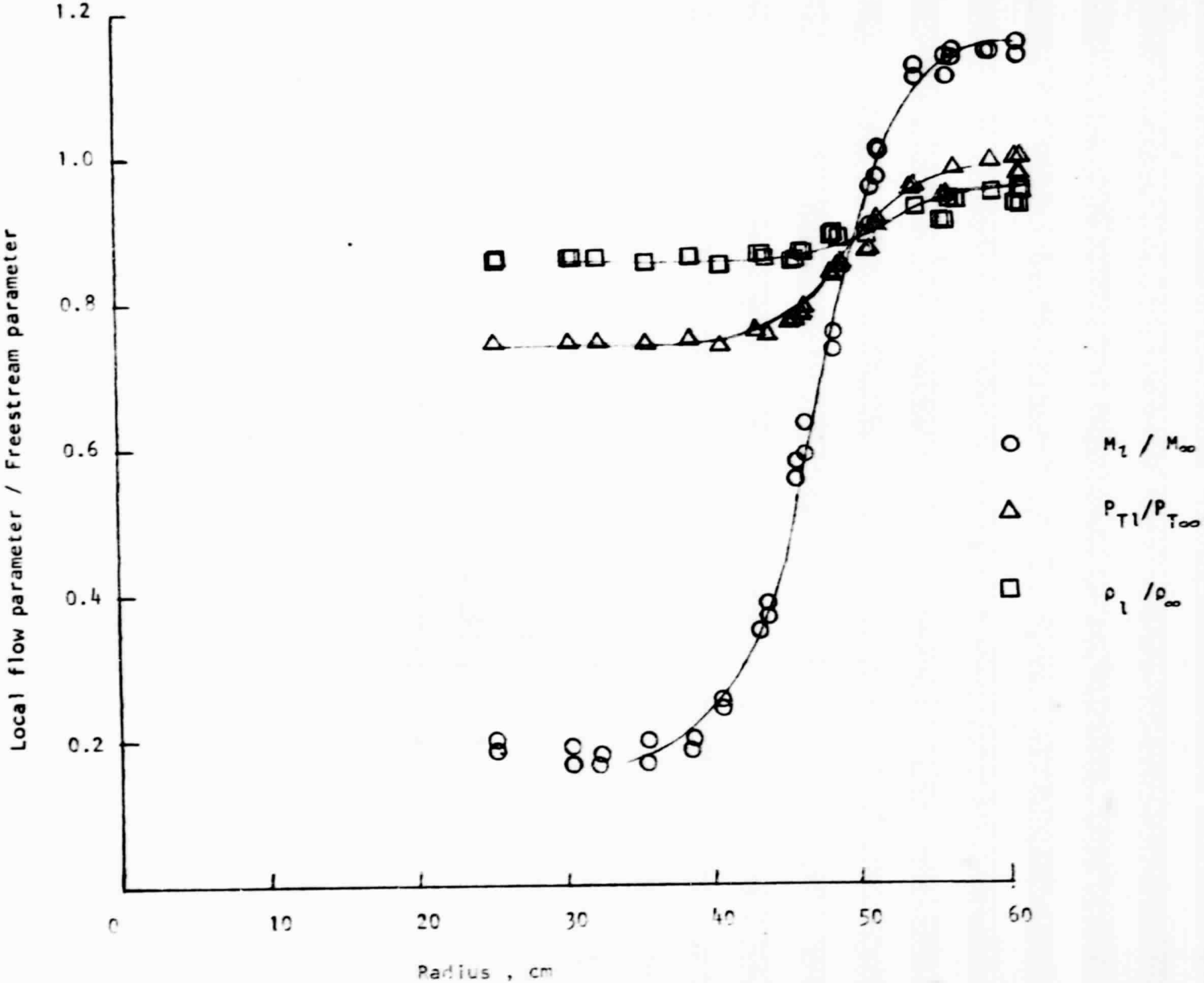

Figure 6. (a) Local Flow Parameter Distribution.
$\theta = 150^\circ$ $M_\infty = 0.55$

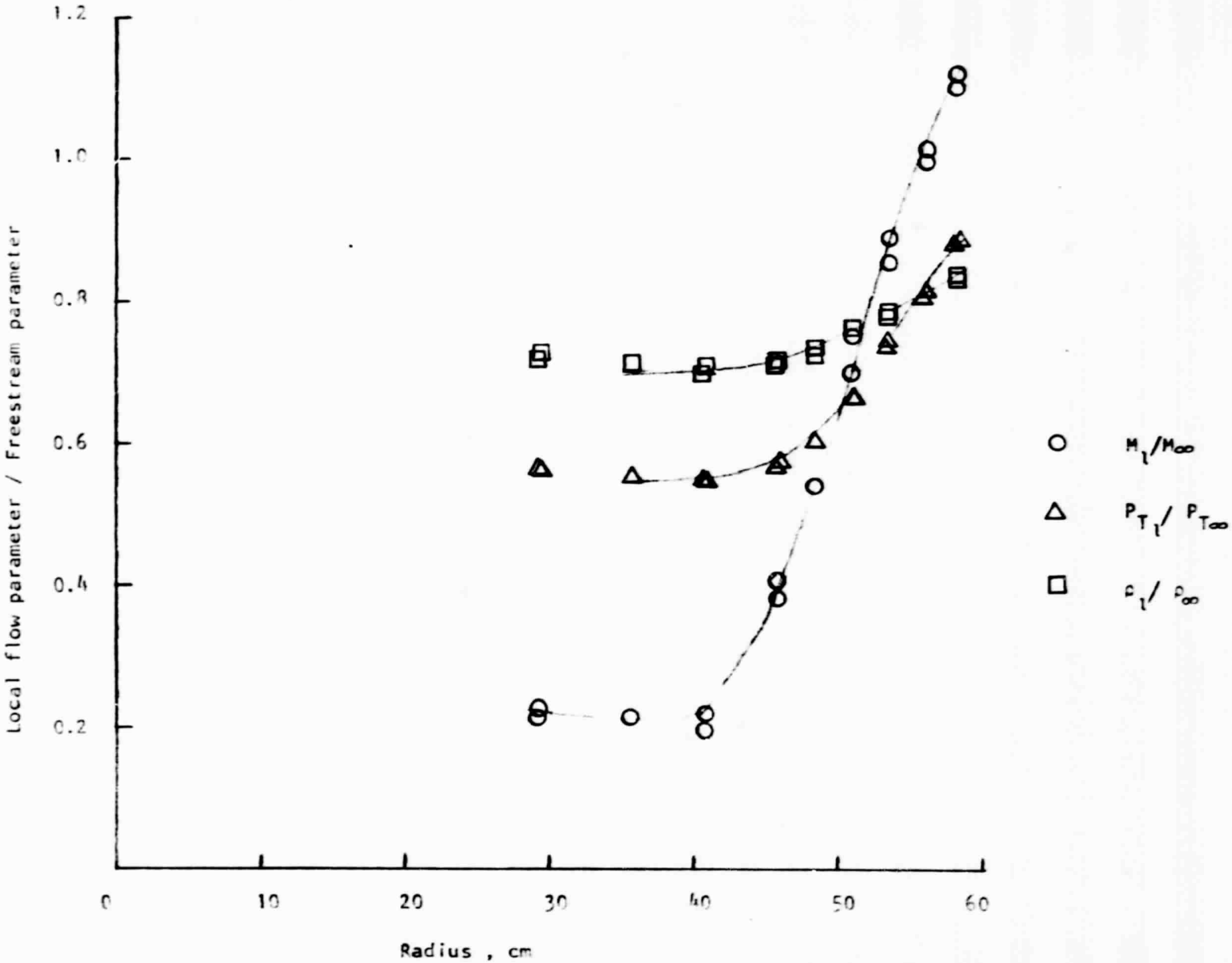

Figure 6. (b) Local Flow Parameter Distribution.
$\theta = 150^0$ M_∞ 0.75

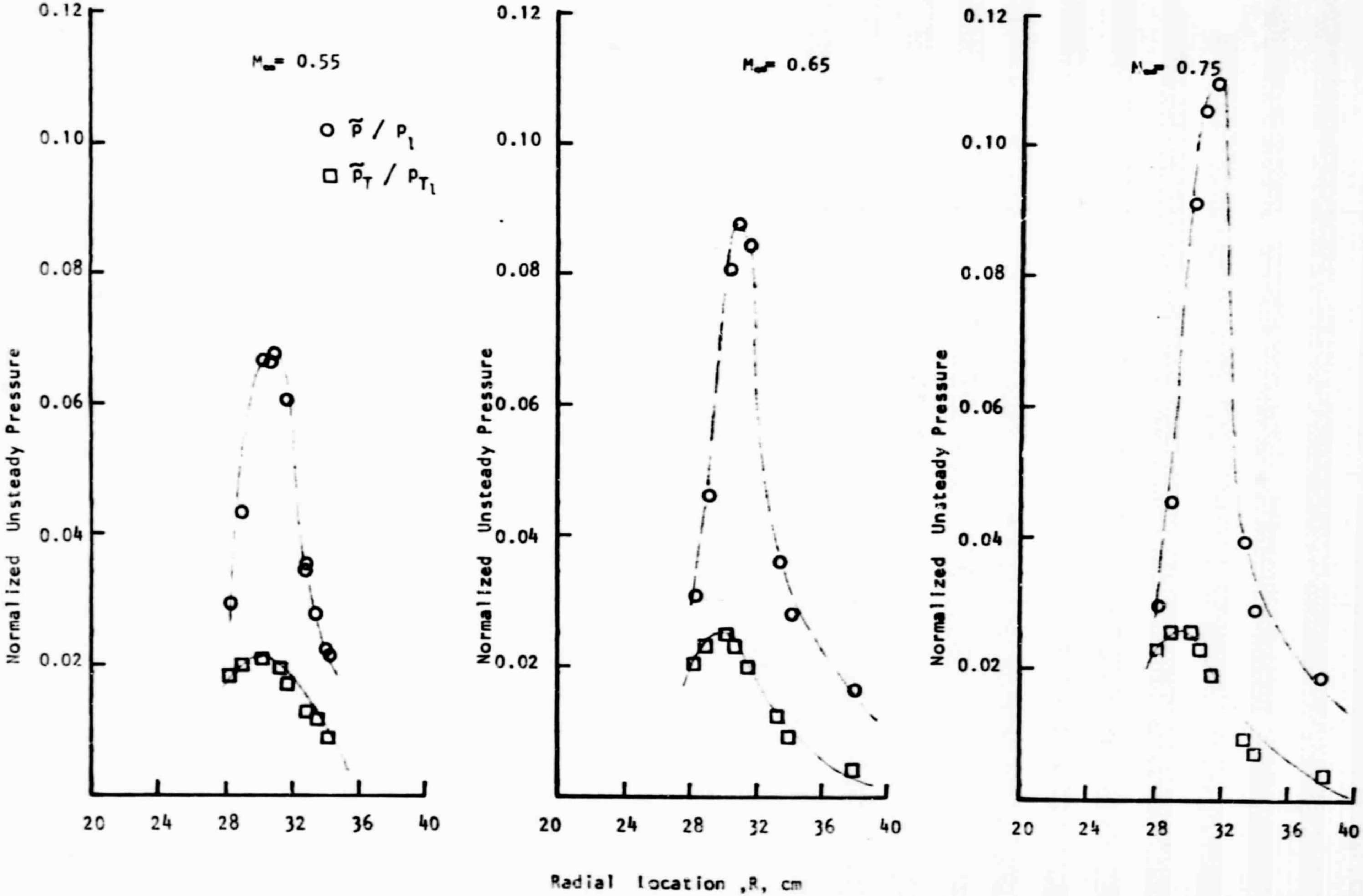

Figure 7. Normalized Unsteady Pressures. Azimuth Angle = 120 deg.

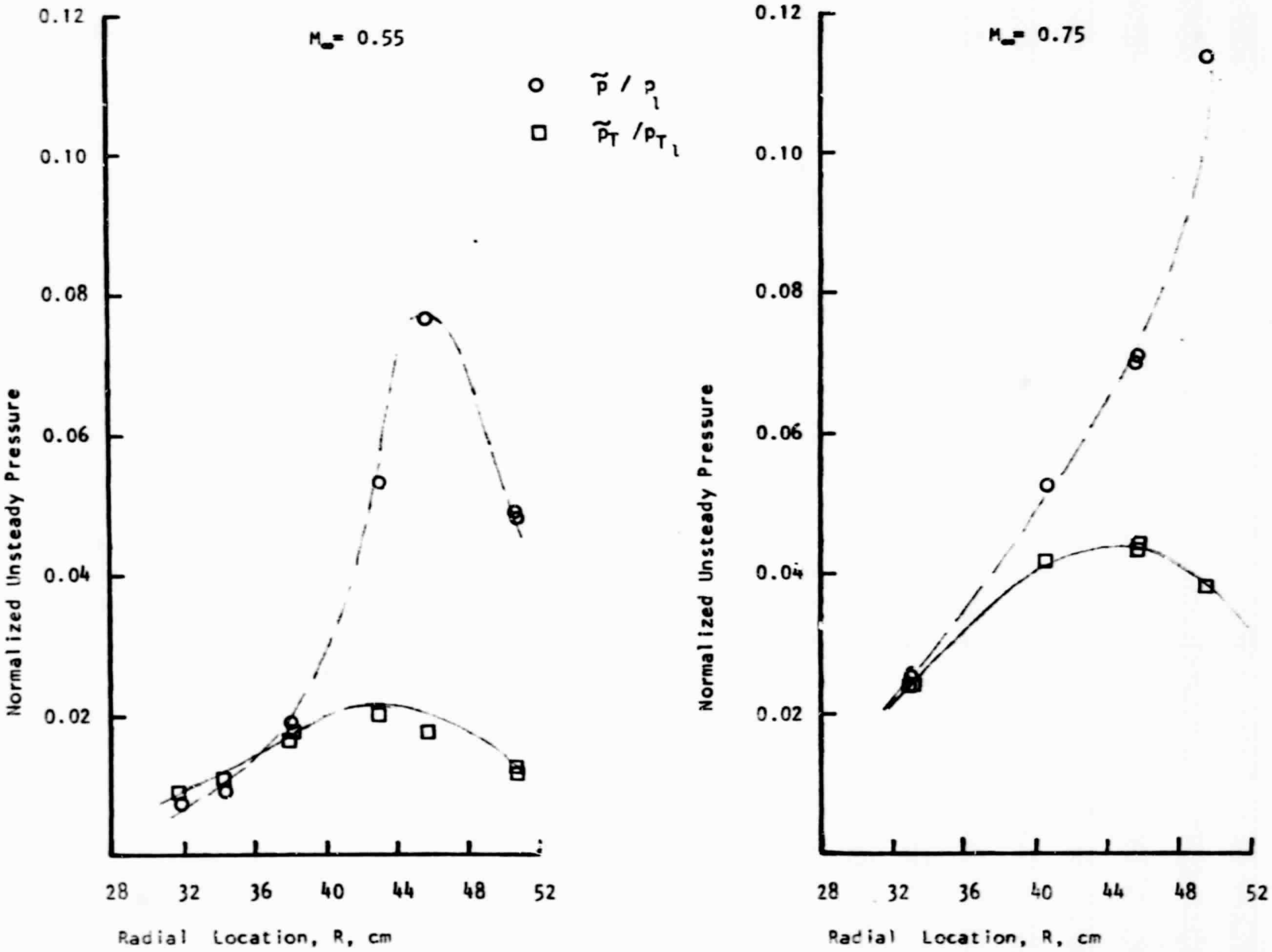

Figure 8 . Normalized Unsteady Pressures. Azimuth Angle = 150 deg.

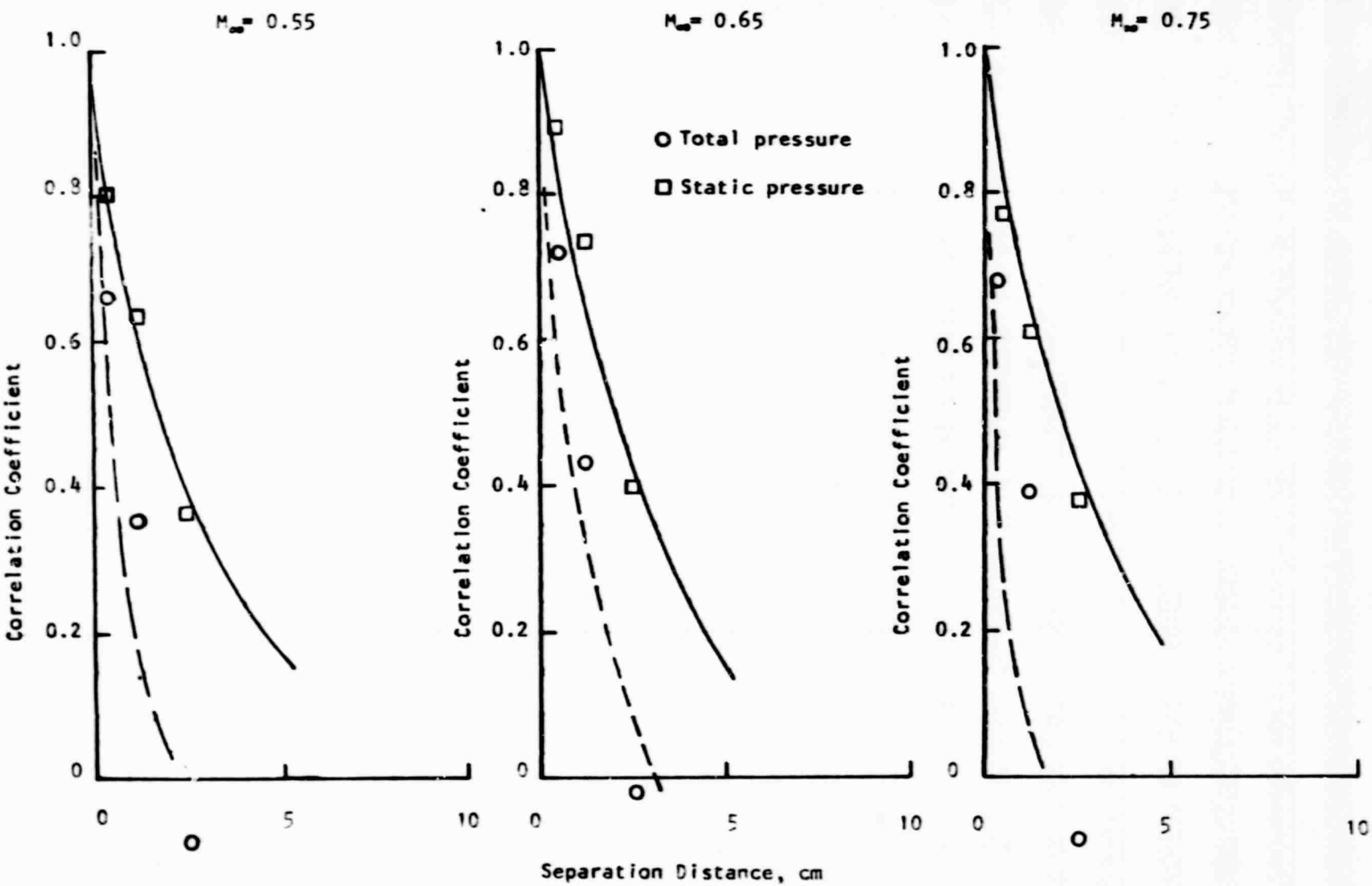

Figure 9. Correlation Coefficients for Azimuth angle =120 degrees (R=28cm)

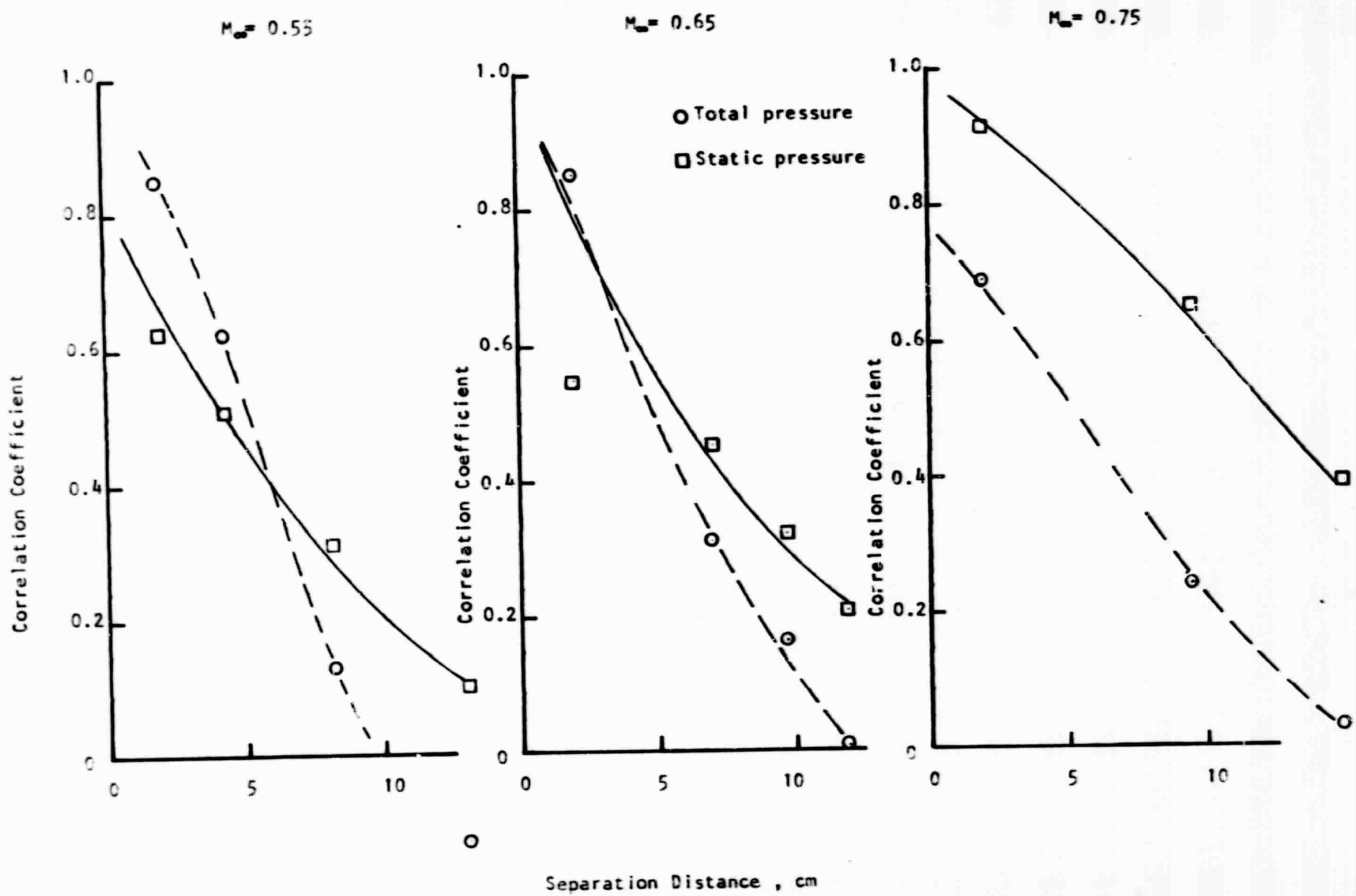

Figure 10 Correlation Coefficients for Azimuth angle = 150 degrees (R=30cm)

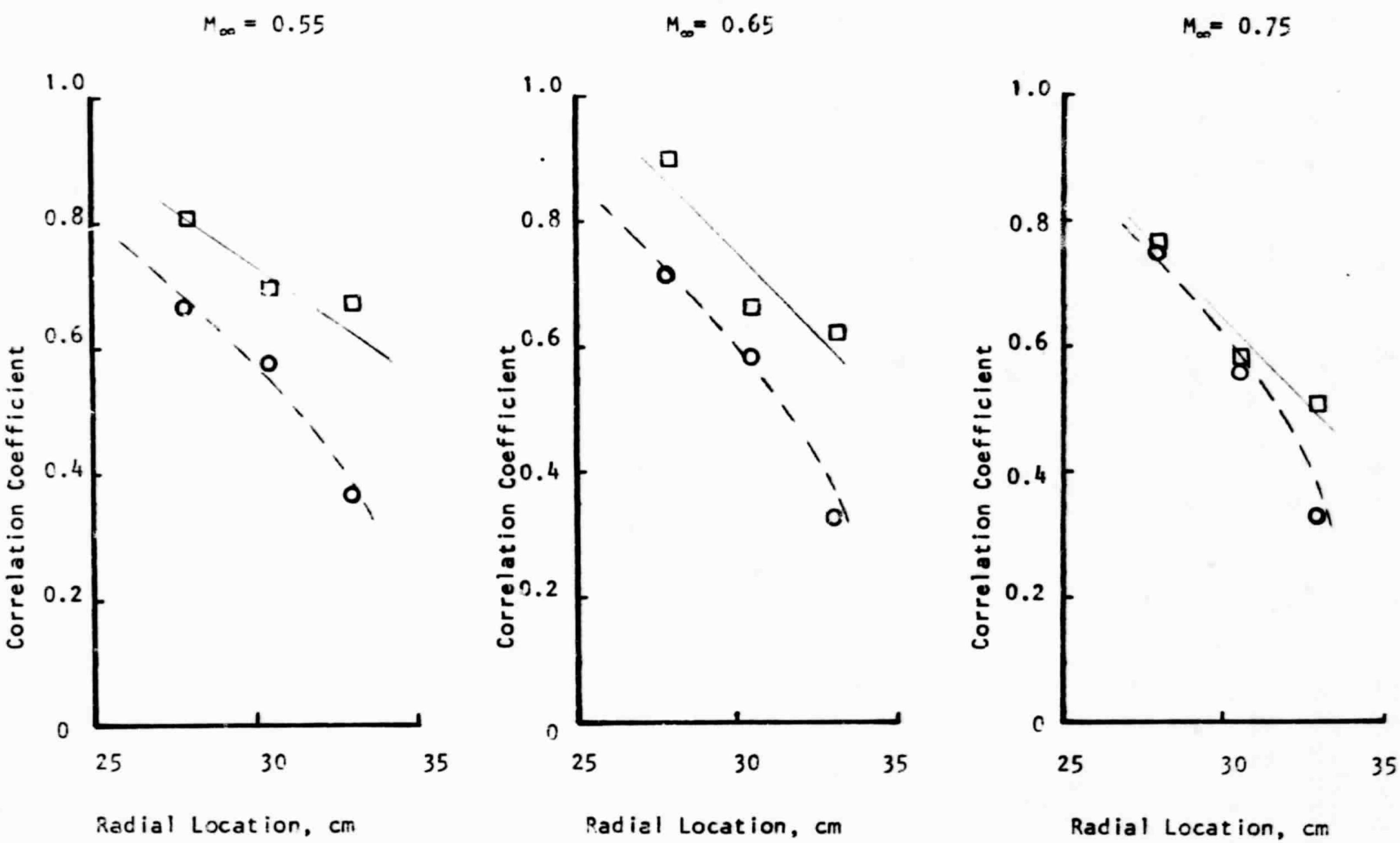

Figure 11. Cross Correlation coefficient versus radial location. $\theta = 120^0$ Separation distance = 0.53 cm.

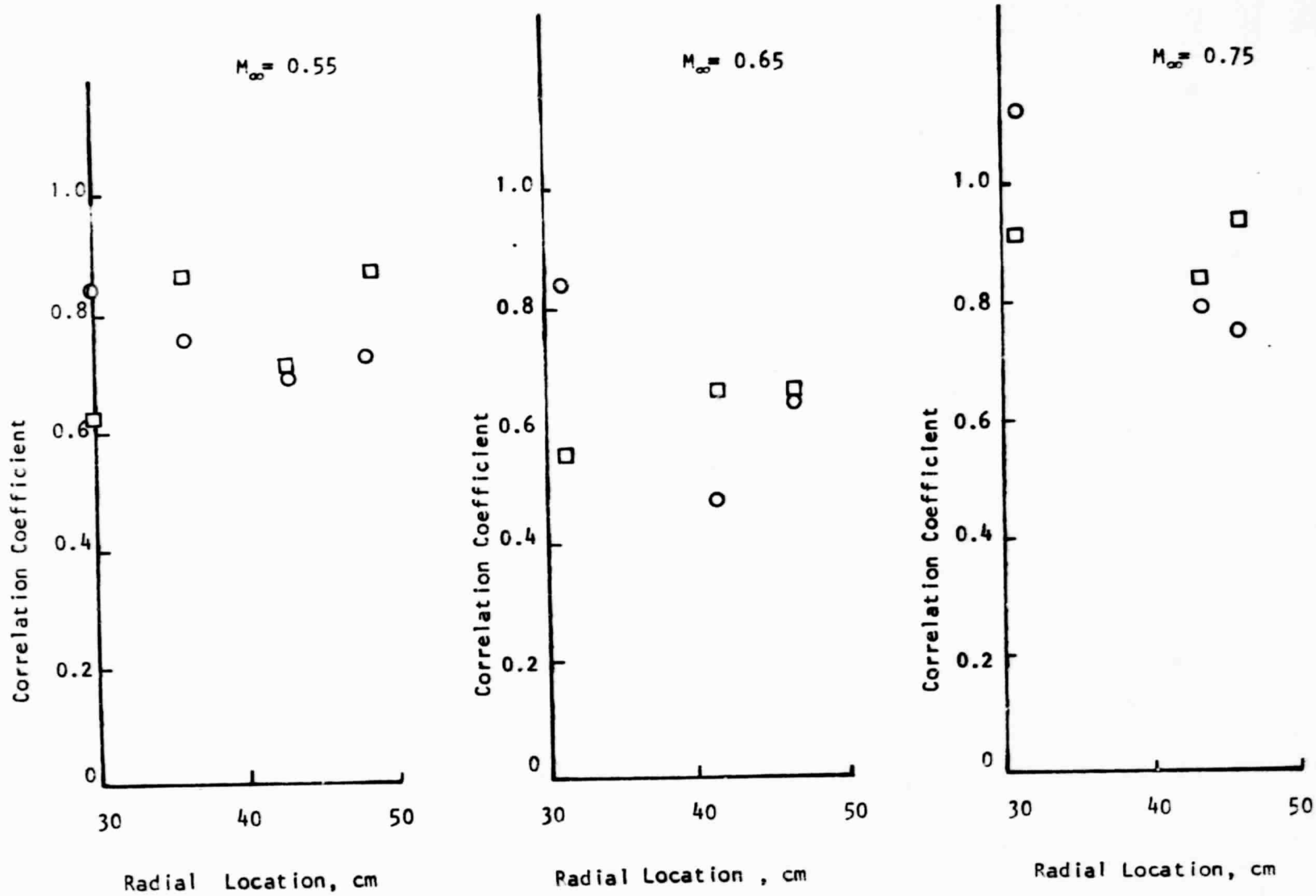

Figure 12. Cross Correlation coefficient versus separation distance.
$\theta = 150^\circ$ Separation distance = 2 cm.